Available online at www.sciencedirect.com
SCIENCE DIRECT®
Chemical Physics Letters 375 (2003) 96–101
CHEMICAL PHYSICS LETTERS
www.elsevier.com/locate/cplett

Bicrystalline zinc oxide nanowires

Ying Dai [a,1], Yue Zhang [a,b,*], Yuan Qiang Bai [a], Zhong Lin Wang [b]

[a] *Department of Materials Physics, State Key Laboratory for Advanced Metals and Materials, University of Science and Technology Beijing, Beijing 100083, China*
[b] *School of Materials Science and Engineering, Georgia Institute of Technology, Atlanta, GA 30332-0245, USA*

Received 1 April 2003; in final form 9 May 2003

Abstract

Bicrystalline ZnO nanowires synthesized are composed of two crystals that form a twin structure parallel to the $(0\,\bar{1}\,1\,4)$ plane with a growth direction closely parallel to $[0\,\bar{1}\,1\,\bar{1}]$ and the $(2\,\bar{1}\,\bar{1}\,0)$ side facet. The twin structure is suggested to be a key factor in leading the axial growth of the nanowire. The photoluminescence spectra of the nanowires show a weak UV emission at 385 nm and a strong green emission at 495 nm. The green emission intensity of the nanowires depends on the different level of oxygen vacancies in the ZnO nanowires.

1. Introduction

One-dimensional (1D) nanostructures, such as nanotubes, nanowires and nanoribbon, have attracted extraordinary attention for their potential applications in device and interconnect integration in nanoelectronics and molecular electronics [1–5]. The semiconducting metal oxide ZnO is a wide band-gap (3.37 eV) compound semiconductor that is suitable for blue optoelectronic applications, with ultraviolet lasing action being reported in disordered particles and thin films [6–9]. One-dimensional single-crystalline ZnO nanostructures have been synthesized successfully in several groups [10–14]. ZnO nanobelts were synthesized at 1350 °C by thermal evaporation of ZnO powders [3,13,14]. The aligned ZnO nanowires grown on an Au-coated sapphire substrate were synthesized with a vapor transport and condensation process [10]. The ZnO nanowires reported in the existing literature are single crystalline except a case in which a single stacking fault along the growth direction was found [3]. Although microtwins boundaries have been observed in both silicon and germanium nanowires [15], the consistent production of bicrystals with a single twin along the growth axis was few. Until very recently, bicrystalline silicon nanowires containing a single twin boundary along the entire length of the growth axis were obtained [16]. In this Letter, we report the synthesis of the bicrystalline ZnO nanowires that have a single twin boundary parallel to the growth axis. The structures, growth mechanism and the optical properties of ZnO nanowires are investigated.

* Corresponding author. Fax: +861062332281.
E-mail addresses: yuezhang@pgschl.ustb.edu.cn (Y. Zhang), daiying@mail.whut.edu.cn (Y. Dai).
[1] Also corresponding author.

0009-2614/03/$ - see front matter
doi:10.1016/S0009-2614(03)00823-6

2. Experimental

2.1. Sample preparation

The ZnO nanowires discussed here were synthesized by thermal evaporation of 99.9% pure zinc powders under controlled conditions without the presence of catalyst. The zinc powders were placed in an alumina tube that was inserted in a horizontal tube furnace, where the temperature, pressure and evaporation time were controlled. The temperature of the furnace was ramped to 850–950 °C at a rate of 50–100 °C/min and kept at that temperature for 10–30 min. The partial pressure of oxygen in the furnace was controlled at low level. During evaporating, the products were deposited onto a silicon substrate placed at the downstream end of the alumina tube.

2.2. Characterization and PL measurement

Structural characterization of the ZnO nanowires was investigated by X-ray diffraction (XRD, D/MAX-RB) with Cu Kα radiation, scanning electron microscopy (SEM,S250-II), transmission electron microscopy (TEM, HP-800) and high-resolution TEM (HRTEM, JEM-2010F). The photoluminescence (PL) measurements were carried out on a HITACHI 4500-type visible–ultraviolet spectrophotometer with a Xe lamp as the excitation light source at room temperature. The excited wavelength was at 310 nm and a 430 nm filter was used.

3. Results and discussion

A typical XRD pattern of ZnO nanowires is shown in Fig. 1a. The diffraction peaks can be indexed to a wurtzite structure of ZnO with cell constants of $a = 0.324$ nm and $c = 0.519$ nm. No diffraction peaks from Zn or other impurities are found in any of our samples within the detection limit. In contrast to the XRD spectra of the ZnO nanowires grown by catalytic synthesis [10,11], wherein the diffraction peaks of the catalyst or the zinc metal appeared with the ZnO peaks, the pure ZnO phase is synthesized on the substrates in our case. The morphology of the as-synthesized products on the substrate is shown in Fig. 1b. The products are straight and uniform ZnO nanowires with a diameter of about 60–250 nm and several hundred micrometers in length. Further structural characterization of the ZnO nanowires is performed by TEM. A low magnification image containing nanowires is shown in Fig. 2a. It is worthy to note that most ZnO nanowires in the sample appear in the form of bicrystallines (as marked by the arrow heads). Fig. 2b presents an enlarged view of a portion of the nanowires, in which the crystal has been slightly tilted to provide contrast between the twin variants. The twin boundary in the bicrystalline is proved by both HRTEM image and electron diffraction pattern, as shown in Fig. 2c. The corresponding electron diffraction pattern along $[2\,\bar{1}\,\bar{1}\,0]$ is shown in Fig. 2d. The pattern is of the wurtzite structure but with a twin in the $(0\,\bar{1}\,1\,4)$ plane, and consists of the

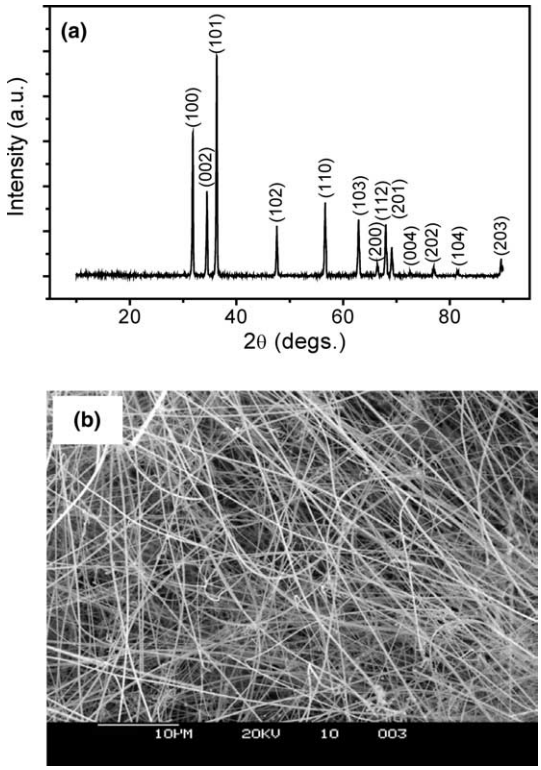

Fig. 1. (a) XRD pattern from the ZnO nanowires. (b) A typical SEM image of the ZnO nanowires.

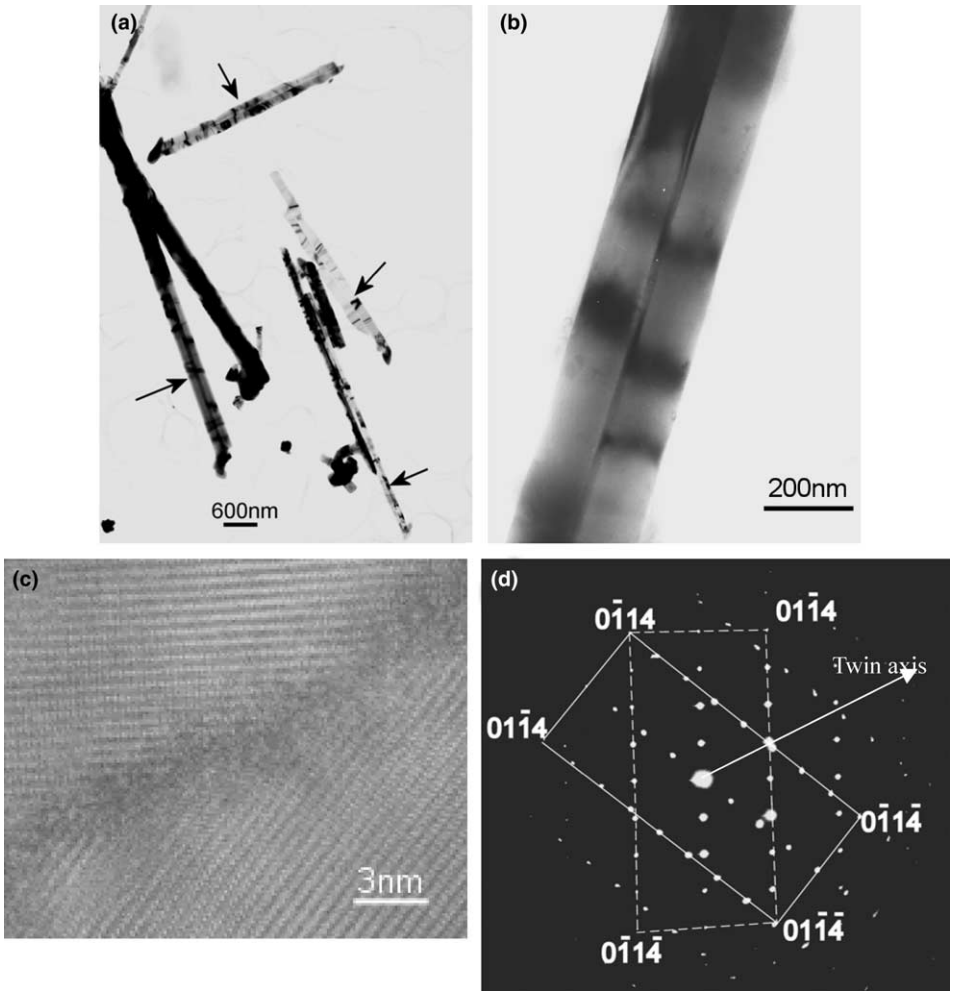

Fig. 2. (a) Low magnification TEM image of ZnO nanowires. The nanowires marked with arrowheads are bicrystalline with a single twin boundary parallel to the long growth axis. (b) A portion of a nanowire at higher magnification. (c) A HRTEM image recorded from the center of the bicrystalline nanowire. (d) Corresponding electron diffraction diffraction pattern from the bicrystalline (singly twinned) nanowire. The incident beam direction is $[2\,\bar{1}\,\bar{1}\,0]$, the twin plane is $(0\,\bar{1}\,1\,4)$.

patterns corresponding to the crystals on both sides of the twin (as indexed). The growth axis of the nanowires is closely parallel to $[0\,\bar{1}\,1\,\bar{1}]$. This is a bicrystalline structured ZnO nanowire.

On the other hand, there is a small quantity of single-crystalline ZnO nanowires in the sample. The direction of growth axis for the nanowire is along [0 0 0 1] (Fig. 3a). Fig. 3b shows a HRTEM image of the nanowire. It reveals that the ZnO nanowire is structurally uniform single crystalline without dislocation. The surfaces of the nanowires are clean, atomically sharp, and without any sheathed amorphous phase. The spacing of 0.26 ± 0.005 nm between adjacent lattice planes corresponds to the distance between two (0 0 0 2) crystal plans, which further proves [0 0 0 1] is the preferred growth direction for ZnO single-crystalline nanowires. This result is the same as that in previous reports for ZnO nanobelts [3,17].

There are a total of four different kinds of nanowire-like structures having been reported for ZnO so far. ZnO nanobelts grow along either [0 0 0 1] or $[0\,1\,\bar{1}\,0]$, while a single stacking is observed for the latter case [3]. Nanowires or nanorods

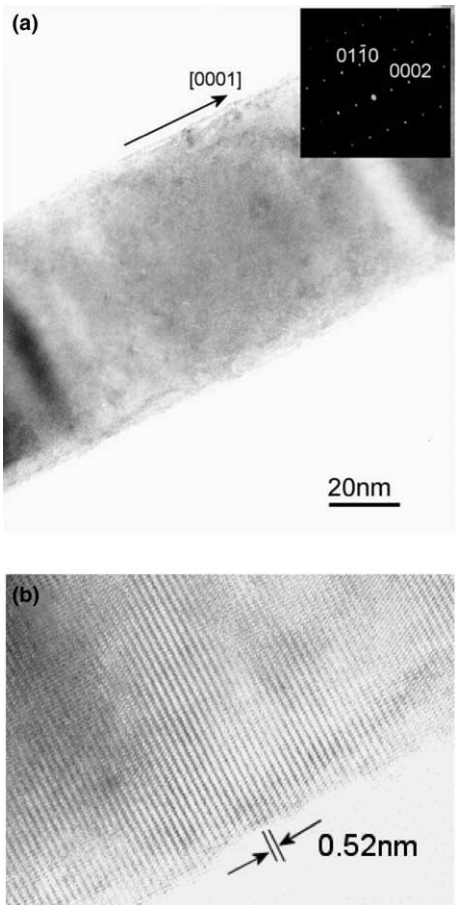

Fig. 3. (a) Low magnification TEM image of a single-crystalline ZnO nanowire. (b) A HRTEM image of a single-crystalline ZnO nanowire. The incident beam direction is [2 $\bar{1}$ $\bar{1}$ 0].

growing along [0 0 0 1] is most often seen [10]. In this Letter, we have demonstrated the synthesis of bicrystalline ZnO nanowires (Fig. 2). The bicrystalline ZnO nanowires contain a single (0 $\bar{1}$ 1 4) twin boundary along the entire length of the [0 $\bar{1}$ 1 $\bar{1}$] growth axis. A common characteristic of these nanostructures is that the (2 $\bar{1}$ $\bar{1}$ 0) plane is a favorable facet.

The formation of nanowires includes two stages: nucleation and growth. ZnO nanowires synthesize in an environment of lower partial pressure of oxygen, different from the tetraleg-ZnO nanorods synthesized in higher partial pressure of oxygen we reported previously [18]. At the initial nucleation stage, Zn vapor might condense onto the substrate in liquid droplet and oxidize to ZnO nuclei afterward. The nucleation is on the silicon substrate, so it is a heterogeneous nucleation process. A typical TEM and HRTEM images recorded from a tip of a bicrystalline ZnO nanowire are shown in Fig. 4. The tip is generally round and consists of a polycrystalline ZnO with twins and defects. The presence of the twin at the tip areas might result in a fast growth of the ZnO nanowire parallel to the twin plane. The irregular shape of the growth front in comparison the

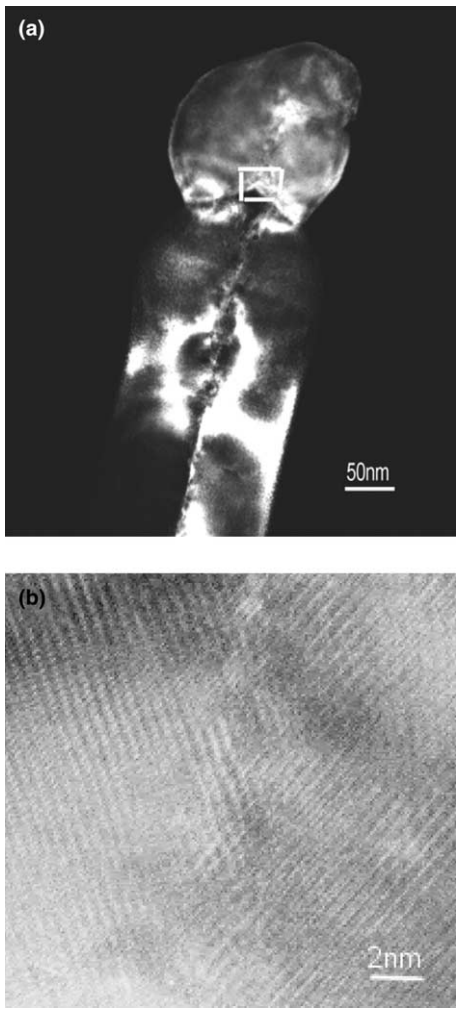

Fig. 4. (a) Low magnification TEM image of a tip of a bicrystalline ZnO nanowire. (b) High-resolution TEM image recorded from the region indicated by a white box in (a).

uniform geometry of the nanowire suggests that the growth front is in liquid state during the growth, which is energetically favorable, and serves as the stable sites for the rapid stacking of incoming atoms. The growth front experienced a rapid oxidation after the temperature dropped and the nanowire exposed to an oxygen rich atmosphere. This means that the VLS process is possible in the growth of the ZnO nanowires. In the present growth of the ZnO nanowires, no additional transition metals are added as catalysts. The formation of the ZnO nanowires might undergo a self-catalyzed VLS growth process [19].

PL spectra of ZnO nanowires at room temperature are shown in Fig. 5. The typical two emission peaks of a narrow peak at 385 nm and a broad peak at 495 nm are observed, which are assigned to the UV emission and green emission, respectively. Whilst the UV emission corresponds to the near band-edge emission, the green emission peak is commonly referred to as a deep-level or trapped-state emission. The green emission is predominant relative to the UV emission at room temperature. Vanheusden et al. [20] attributed the green transition to the singly ionized oxygen vacancy in ZnO and suggested the emission coming from the radiative recombination of a photon generated hole with an electron occupying the oxygen vacancy. This model is fully supported by our results as follows: the ZnO nanowires are synthesized in an environment of lower partial pressure of oxygen, i.e., the nanowires are formed in an oxygen lacking environments. Oxygen vacancies are formed in growth of ZnO nanowires, resulting in the formation of non-stoichiometric phase structures. Therefore, strong green light emission from the nanowires is observed (in Fig. 5a). When the nanowires are treated at 950 °C for 1 h in air after the growth, the concentration of oxygen vacancies decreases. The green emission intensity of the nanowires is decreased dramatically, as shown in Fig. 5b. The more singly ionized oxygen vacancies there are, the stronger the intensity of the green luminescence is. The weaker green light emission from the treated nanowires is related to the reduced oxygen vacancy concentration. It is obvious that optical property of the ZnO nanowires is tunable by controlling the oxygen vacancy concentration [21]. The electronic property of ZnO nanobelt can be tuned from semiconductor to metallic by introducing oxygen vacancies [22]. The relation between the intensity of green light emission and the concentration of the oxygen vacancy in ZnO nanowires is also being investigated by positive electron annihilation technique (PAT) in our group.

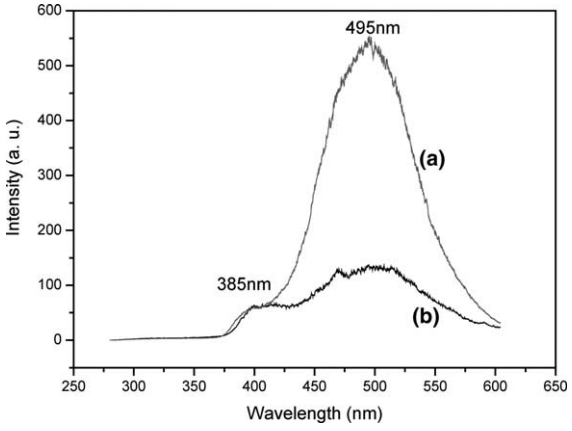

Fig. 5. Photoluminescence spectra of ZnO nanowires at room temperature: (a) before heat treatment and (b) after heat treatment at 950 °C air for 1 h.

4. Conclusions

We have synthesized bicrystalline ZnO nanowires by oxidation of Zn powders. TEM and HRTEM investigations show that the nanowires are composed of two crystals that form a twin structure parallel to the $(0\,\bar{1}\,1\,4)$ plane with a growth direction closely parallel to $[0\,\bar{1}\,1\,\bar{1}]$ and the $(2\,\bar{1}\,\bar{1}\,0)$ side facet. The nanowires are generally free from dislocations. The optical property of the ZnO nanowires varies with the different level of oxygen vacancies in them. These unusual structures offer a model system for studying of charge and mass transport across/along a single planar defect.

Acknowledgements

The work was supported by the National Natural Science Foundation of China (Grant Nos.

50232030 and 50172006), the Fund for Returned Overseas Scholar of Ministry of Education of China, the Fund for Cross-Century Talent Projects of Educational Ministry of China and the Research Fund for the Doctoral Program of Higher Education of China.

References

[1] R.H. Baughman, A.A. Zakhidov, W.A. Hee, Science 297 (2002) 787.
[2] J. Hu, T.W. Odom, C.M. Lieber, Acc. Chem. Res. 32 (1999) 435.
[3] Z.W. Pan, Z.R. Dai, Z.L. Wang, Science 291 (2001) 1947.
[4] J.R. Heath, P.J. Kuekes, G. Synder, R.S. Williams, Science 280 (1998) 1717.
[5] D. Snoke, Science 273 (1996) 1351.
[6] D.M. Bagnall, Y.F. Chen, Z. Zhu, T. Yao, S. Koyama, M.Y. Shen, T. Goto, Appl. Phys. Lett. 70 (1997) 2230.
[7] P. Zu, Z.K. Tang, G.K.L. Wong, M. Kawasaki, A. Ohtomo, H. Koinuma, Y. Segawa, Solid State Commun. 103 (1997) 459.
[8] H. Co, J.Y. Xu, E.W. Seelig, R.P.H. Chang, Appl. Phys. Lett. 76 (2000) 2997.
[9] D.Z. Zhang, S.H. Chang, S.T. Ho, E.W. Seelig, X. Liu, R.P.H. Chang, Phys. Rev. Lett. 84 (2000) 5584.
[10] M.H. Huang, Y. Wu, H. Feick, N. Tran, E. Weber, P. Yang, Adv. Mater. 13 (2001) 113.
[11] Y.C. Kong, D.P. Yu, B. Zhang, W. Feng, S.Q. Feng, Appl. Phys. Lett. 78 (2001) 407.
[12] W.I. Park, D.H. Kim, S.W. Jung, G.C. Yi, Appl. Phys. Lett. 80 (2002) 4232.
[13] Z.L. Wang, R.P. Gao, Z.W. Pan, Z.R. Dai, Adv. Eng. Mater. 3 (2001) 657.
[14] Z.R. Dai, Z.W. Pan, Z.L. Wang, Solid State Commun. 118 (2001) 351.
[15] Y.J. Han, J. Kim, G.D. Stucky, Chem. Mater. 12 (2000) 2068.
[16] C.C. Chen, C.Y. Chao, Z.H. Lang, Chem. Mater. 12 (2000) 1516.
[17] M.H. Huang, S. Mao, H. Feick, H. Yan, Y. Wu, H. Kind, E. Weber, R. Russo, P. Yang, Science 292 (2001) 1897.
[18] Y. Dai, Y. Zhang, Q.K. Li, C.W. Nan, Chem. Phys. Lett. 358 (2002) 83.
[19] J.Q. Hu, Q. Li, N.B. Wong, C.S. Lee, S.T. Lee, Chem. Mater. 14 (2002) 1216.
[20] K. Vanheusden, W.L. Warren, C.H. Seager, D.R. Tallant, J.A. Voigt, B.E. Gnade, J. Appl. Phys. 79 (1996) 7983.
[21] Z.L. Wang, Z.C. Kang, Functional and Smart Materials – Structural Evolution and Structure Analysis, Plenum Press, New York, 1998.
[22] M. Arnold, P. Avouris, Z.W. Pan, Z.L. Wang, J. Phys. Chem. B 107 (2003) 659.